RESEARCH BULLETIN 855 MARCH 1964

UNIVERSITY OF MISSOURI COLLEGE OF AGRICULTURE
AGRICULTURAL EXPERIMENT STATION
ELMER R. KIEHL, *Director*

Characteristics of Flow in Trapezoidal and Triangular Irrigation Furrows

JOHN F. THORNTON
Corn Belt Branch
Soil & Water Conservation Research Division
Agricultural Research Service
U. S. Department of Agriculture
and
ROBERT P. BEASLEY
Agricultural Engineering Department
Missouri Agricultural Experiment Station
Columbia. Missouri

(Publication authorized March 27, 1964)

COLUMBIA, MISSOURI

ABSTRACT

The hydraulics of flow in furrow irrigation is a field in which little directly applicable basic research has been done. The purpose of this study was to investigate the characteristics of flow in irrigation furrows, as influenced by furrow shape, roughness, slope, and rate of flow.

Hydraulic tests were conducted in a flume 30 feet long, 3.33 feet wide, and 1.66 feet deep. Furrows with trapezoidal and triangular shapes were formed in the flume.

Tests were run on four different roughnesses, using five rates of flow and six slopes. The furrows were constructed of aluminum and lined with silt or sand to provide different degrees of roughness. Additional tests were run using furrows of the above-mentioned shapes formed in soil. During one series of tests, water was removed from the soil by a vacuum system to maintain infiltration. Another series was run without infiltration. Tests on furrows in soil were also run with five rates of flow and six slopes.

Data from the hydraulic tests were analyzed to determine the relationship between the roughness coefficient and the following variables: (1) the velocity, (2) the depth, (3) the hydraulic radius, and (4) the Reynolds number. These results are presented graphically.

Results of the investigation indicated that:

1. The roughness coefficient was a function of the velocity, depth, hydraulic radius, and Reynolds number. The roughness coefficient decreased with an increase in each of these four variables.
2. The roughness coefficient was higher for the trapezoidal furrow than for the triangular furrow with the same rate of flow, degree of roughness, and slope.
3. The Reynolds number was three to eight times higher for the triangular furrow than for the trapezoidal furrow with the same rate of flow, degree of roughness, and slope.
4. The average infiltration rate was 0.12 inch per hour for the trapoizoidal furrow and 0.87 inch per hour for the triangular furrow. The differences in infiltration rates in the two furrows can be explained by the differences in depth of flow, deposition of sediment, and the ratio of wetted perimeter to width of water surface.

CONTENTS

This bulletin is a report on Department of Agricultural Engineering research project 395, "Use of Water." Work was done in cooperation with the Corn Belt Branch, Soil and Water Conservation Research Division, Agricultural Research Service, USDA.

Characteristics of Flow in Trapezoidal and Triangular Irrigation Furrows

John F. Thornton and Robert P. Beasley

INTRODUCTION

Water is one of our major national concerns. Throughout the nation, water requirements for agriculture, industry, and municipalities have increased steadily. Concomitant with this increased requirement comes more intense competition for the available supplies and demands for the reduction of losses and more efficient reuse of water. Water for irrigation must not only be used more efficiently, but must be managed to eliminate soil erosion and waterlogging, if irrigation development is to be productive and permanent.

With more emphasis being placed on the efficiency of water use for irrigation, a study of the hydraulics of furrow irrigation becomes increasingly important. Empirical methods now commonly used in the design of furrow irrigation systems involve flow phenomena that are extremely complex. The complexity of these flow phenomena has been recognized, but in most cases it has been underestimated.

Significant progress in defining the hydraulics of furrow irrigation is inseparably connected to the degree with which the investigator understands and uses the fundamental physical aspects of the flow. Knowledge of the relationship between rate of flow, velocity, furrow shape, infiltration rate and roughness will enable the designer to improve uniformity of water distribution with a minimum of erosion.

REVIEW OF LITERATURE

The original equation relating the rate of flow in open channels to the characteristics of the channel was suggested by Chezy in 1775 (8) and is still used. This equation is usually written

$$V = C\sqrt{RS}$$

where $\underline{V}$ is the mean velocity, $\underline{R}$ is the hydraulic radius, $\underline{S}$ is the slope of the energy line, and $\underline{C}$ is a factor of flow resistance, Chezy's limited data indicated that $\underline{C}$ was a constant. Later scientists recognized that $\underline{C}$ was a function of slope, hydraulic radius, and the degree of roughness.

The Manning equation was presented in 1889. This equation was originally written

$$V = KR^{2/3}S^{1/2}$$

and is now usually expressed as

$$V = \frac{1.486}{n} R^{2/3}S^{1/2}$$

where V is the mean velocity, R is the hydraulic radius, S is the slope of energy line, and n is a characteristic of the roughness of the boundary material (8). The Manning equation is the most used open-channel flow equation.

Other open-channel flow equations were published by Ganguillet and Kutter and Bazin in the 19th century. These equations do not have widespread usage (4).

Early investigators noted the existence of two different types of flow in open channels --- laminar and turbulent. Reynolds in 1883 discussed a rational parameter to distinguish the limit between the two types of flow (8). He believed the development of eddies in pipe flow would vary directly with velocity and pipe diameter and with the ratio of fluid density to fluid viscosity. The parameter, called "Reynolds number", is

$$Re = \frac{VL}{\nu}$$

where V is the average velocity, L is a length factor and ν is the kinematic viscosity. The hydraulic radius is the length factor used for flow in open channels.

The irrigation engineer is interested in the Reynolds number which distinguishes the lower limit of turbulent flow. Unfortunately, disagreement exists concerning the Reynolds number where the flow changes from laminar to turbulent in open channels.

Owen (5) conducted flow studies in a glass-walled flume with a polished brass floor 1.5 feet wide and 20 feet long. The slopes and flow depths were not presented. The presence of laminar or turbulent flow was determined from the relationships of Reynolds number and friction factor, and by injecting a stream of dye into the flow. Owen indicated that the flow changed from laminar to turbulent at a Reynolds number of about 1,000. His results could be questioned because uniform flow probably did not exist and velocity distribution had probably not stabilized, since flow in an open channel is actually three dimensional as opposed to the assumed two dimensional flow, and the Reynolds number is dependent upon channel shape.

Horton, Leach, and Van Vliet (3) studied flow in a smooth wooden flume 5.6 inches wide and 34.8 inches long. The flow depths used were from 0.005 to 0.015 foot, and the slopes ranged from 0.07 to 0.25 per cent. They questioned the use of the Reynolds number as the only criterion of flow regime in open channels and suggested a calculated critical velocity for a given channel roughness and flow depth. They reported that flow changed from laminar to turbulent at a Reynolds number of about 550 for their tests.

Parsons (6) studies laminar, transition, and turbulent flow in a channel with a concrete bottom 2 feet wide and 8 feet long. He questioned the use of the hydraulic radius as the length factor in calculating the Reynolds number for laminar sheet flow, and developed a modification of the laminar flow equation to represent disturbed viscous flow.

Powell (7) examined the effect of discharge, roughness and slope on the flow. He suggested that, in channels, the transition from laminar to turbulent flow may be so abrupt that characterization of the transition zone may not be a problem. Powell's studies did not include the extreme magnitude of relative roughness likely to be found in channels comparable to irrigation furrows.

MATERIALS, EQUIPMENT, AND PROCEDURE

The purpose of this study was to investigate the characteristics of flow in irrigation furrows, as influenced by furrow shape, slope, roughness, infiltration rate, and rate of flow. The characteristics of flow in furrows were determined in the fall of 1961 and spring of 1962 in an indoor hydraulics laboratory, which consisted of a circulated water supply, a hydraulic flume, and related equipment. The aluminum furrows tested were trapezoidal and triangular. Tests were run on four different roughnesses, using five rates of flow and six slopes. Additional tests were run with five rates of flow and six slopes, using furrows of the shapes mentioned above formed in soil. During one series of tests, water was removed from the soil by a vacuum system to cause infiltration. Another series was run without infiltration.

Physical Tests of the Soil

Infiltration was considered the most important soil property in a study of the interactions of flowing water over soils. The soil selected was a silt loam taken from the 6- to 18-inch subsurface layer of Knox silt loam.

Mechanical analysis: The particle-size distributions of the soil sample were determined in accordance with procedures outlined by the American Society for Testing Materials, and three additional hydrometer readings were made at 15-, 30-, and 40-second intervals (1), See Figure 1.

Stability of soil aggregates: In studying the properties of a soil that influence the interactions of water flowing over and into soils, investigators have determined the structural stability of soil aggregates in water.

There is no single accepted method of aggregate analysis. The aggregate analysis data reported here were determined by a modified hydrometer method as follows. A sample of the Knox silt loam was per-

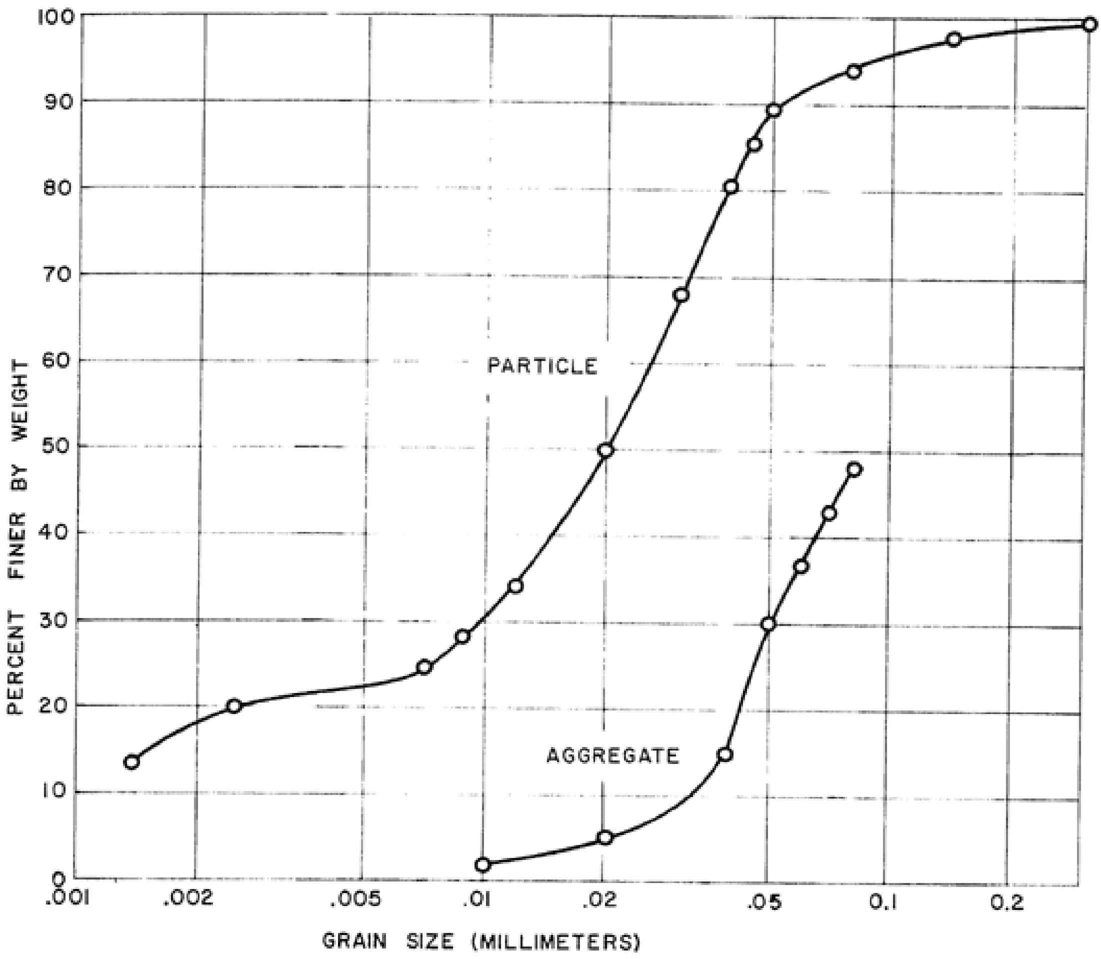

Fig. 1-Particle size and aggregate size distribution curves for Knox silt loam.

mitted to dry slowly and, when sufficiently friable, was passed gently through an 8-mm. sieve and air dried. A sample of approximately 100 gms. was weighed and placed in a plexiglass graduate, 2.5 inches in diameter and 18 inches in height, which was filled to the 1 liter mark with distilled water. The graduate was inverted at 10-second intervals for 100 seconds and then at 5-second intervals for 60 seconds. Hydrometer readings were then made at the end of 15, 30, and 40 seconds, and at 1, 2, 5, 15, 30, and 60 minutes. The results of the hydrometer tests were analyzed by the procedure given by the American Society for Testing materials (1). The aggregate-size curve is shown on the same drawing as the partical-size curve. See Figure 1.

Hydraulic Test

Details of the hydraulic flume and related apparatus, as well as experimental procedure for determining the characteristics of flow in the irrigation furrow, are given in the following sections.

Hydraulic flume. The hydraulic flume was 30 feet long, 3.33 feet wide, and 1.66 feet deep. The flume was constructed of sheet aluminum 0.0625 inch thick, with aluminum and wood structural members used for framing and for edge flanges of the flume. The flume was constructed on two tubular steel beams 28 feet long which were, in turn, supported by a pivot point 8 inches upstream from the center of the beams and by a pair of mechanical screw jacks placed at each end of the beams. The support arrangement permitted the slope of the flume to be varied from zero to approximately 2 percent. The trapezoidal and triangular furrows (Figure 2) were constructed of sheet aluminum 0.0625 inch thick. Both furrows were 6 inches deep with 1.5 to 1 side slopes, and the trapezoidal furrows had 20-inch bottoms. Furrows with the same shapes were also constructed in silt loam soil.

At the upstream end of the flume, a stilling basin was constructed of stainless steel and attached to the flume with an adjustable approach channel 42 inches long, with 1.5 to 1 side slope, and a 20-inch bottom. The stilling basin was 3 feet square and 6 feet high, with a slotted side so that the delivery height of the approach channel might be changed when the slope of the model was altered. To aid in dissipating the turbulence of the incoming flow, the inlet was in the bottom of the stilling basin.

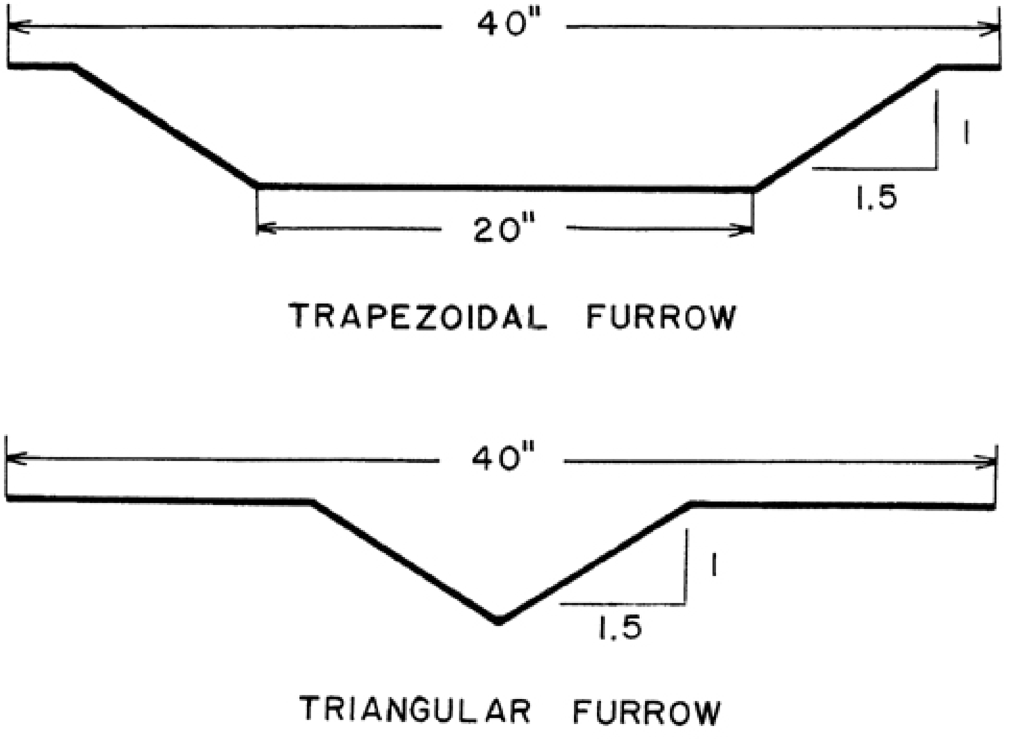

Fig. 2-Furrow shapes used in the tests.

At the outlet end of the flume, a vertically sliding, slotted tail gate was attached. By manipulation of this tail gate, the depth of flow at the outer end of the flume could be controlled. To obtain a condition approaching uniform flow in the flume, the tail gate was adjusted so that the water-surface profile was parallel to the channel bed.

Piezometers were attached in the center of the flume on 2-foot centers, starting at a distance of 2 feet from the upstream end of the flume. The piezometer board consisted of 14 Pyrex glass tubes, which were 8 mm. in inside diameter and 24 inches long, mounted on a plywood board. The piezometer scales were located such that the depth of water at that point in the flume could be read directly.

Later, a system to provide suction in the soil was installed on the bed of the trapezoidal furrow in the flume. This system consisted of five parallel lines of porous ceramic tubes laid on 5-inch centers across the width of the bed on about 1/4 inch of soil. The individual ceramic tubes were approximately 12 inches long, 0.8-inch O.D. X 0.55-inch I.D., connected with 3/4-inch I.D. clear plastic tubing. The ceramic tubes used were capable of removing about 1.5 to 2.0 mm. of water per minute for each 12-inch tube from saturated soil, with a suction of approximately 0.8 atmosphere. Since the air entry value of the ceramic tubes was about 0.85 atmosphere or greater, 0.8 was used as the operating basis. Each line of ceramic tubes was connected to a 5-gallon jug and the jugs were connected in parallel to a vacuum system by means of tygon tubing.

The flume was filled with a Knox silt loam soil to a 15-inch depth over the porous tubes. Trapezoidal and triangular furrows with the same dimensions as the aluminum furrows were made in the soil, using a specially constructed template.

Water supply. A tank 3 feet wide, 3 feet deep, and 6 feet long, on which an HS-type flume was mounted, contained the water supply. This tank was filled to approximately three-fourths of its capacity and allowed to adjust to ambient temperature. The water was pumped from the tank, through pipe and flow meters, into the bottom of the stilling basin, and through the approach channel to the furrow. A valve was located on the pressure side of the pump, enabling accurate control of the flow. The water from the furrow returned through the HS-type flume to the starting point in the tank.

Flow-rate measurements. The rate of flow into the stilling basin was measured with a 3/4-inch meter, located in the supply line, just before entry into the stilling basin. The rate of flow out of the furrow was measured by a 1-foot HS-type measuring flume developed by the U.S. Soil Conservation Service (2). The meter and the HS-type flume were calibrated.

The HS-type flume was located on the water supply tank. The head on this flume was measured by a float-type water level recorder, so that flow measurements were made continuously. A schematic drawing of the equipment is shown in Figure 3.

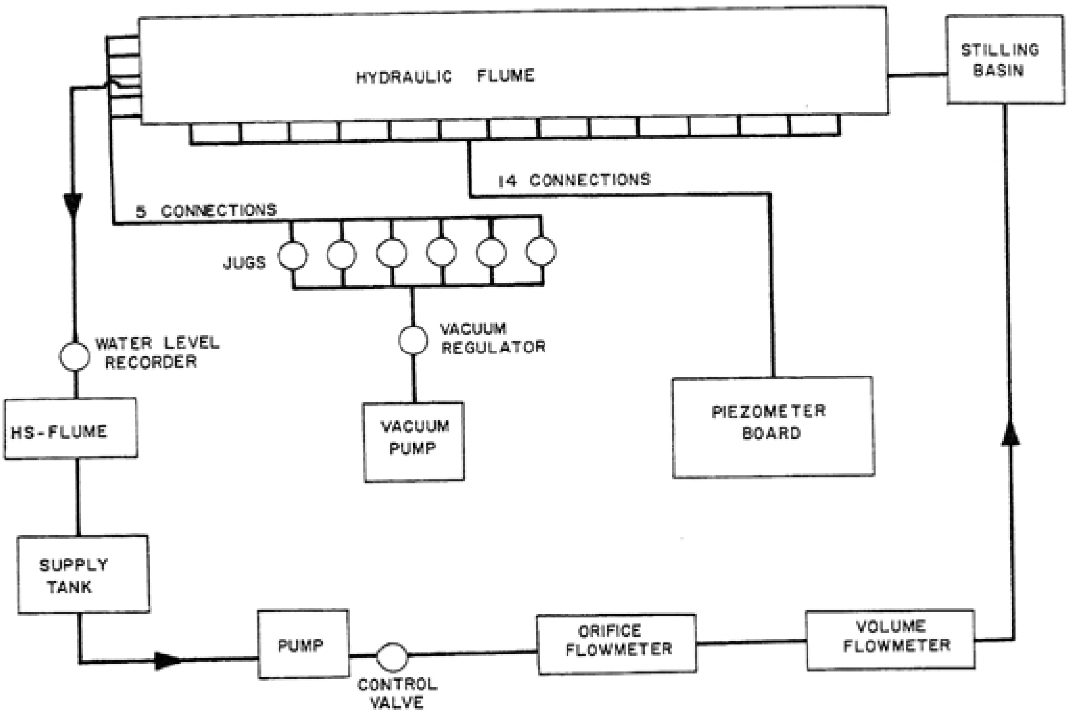

Fig. 3-Schematic drawing of the hydraulic flume and related apparatus.

Depth measurements: A point gage was used in all the measurements of depth. It was mounted on a moveable frame and could be moved to three locations along the furrow. The depth of flow was determined at 12, 18, and 24 feet from the upstream end of the furrow. The difference between the channel elevation and the water surface at a given point constituted the depth of flow at that point.

Any depth measurement could be satisfactorily duplicated to the 0.001 foot with the apparatus previously described. Although there were slight rapid fluctuations on the water surface itself, probably caused by turbulence, these could be averaged quite accurately by eye.

Furrow Roughness. Four degrees of roughness were produced by the use of smooth aluminum and by coating smooth aluminum with 44-micron silica, 715-micron silica, and 1500-micron silica.

For the roughness tests, the furrows were lined with silt or sand imbedded in a coating of asphalt roofing paint. First, the 44-micron silt was applied to a coat of asphalt roofing paint on the smooth aluminum. The 715-micron sand was applied the same way on top of the silt. Likewise, the 1500 micron sand was applied on top of the two finer layers.

Furrow shapes in soil. The influence of furrow shapes in soil was studied, using Knox silt loam. The soil was thoroughly screened and mixed. Lumps of soil were broken up by hand on a 1/2-inch screen and all coarse, foreign particles were removed. Approximately 10,000 pounds of soil were used to fill the flume to about a 1.5-foot depth over the ceramic tubes. The furrow was then carefully shaped and leveled lengthwise, with a template that used the sides of the flume as guides. No attempt was made to compact the soil any more than that which naturally occurred in the process of filling and forming the furrow. The soil was then wetted by slowly admitting water into the furrow until all the soil in the flume was saturated. A layer of soil, more than enough to take care of the settling, was applied and rewetted.

The soil was dried by applying a suction in the porous tubes and by blowing air from a fan over the furrow surface. When the furrow was dry enough to work, the template was used again to reshape the furrow for the test. The bulk density obtained was 1.35 gm. per cc.

Tests in the furrow. Before beginning the actual test the piezometers were checked for clogging, a chart was placed on the clock in the water level recorder to measure the height of flow in the HS-type flume, and the temperature of the water was recorded.

At the beginning of the test, the pump was started and the flow was adjusted to a preselected rate by the use of the control valve. If the depths of flow along the furrow as measured by the piezometers indicated nonuniform flow, the tailgate was adjusted to establish uniform flow.

The rate of flow into the furrow was determined from the gallons recorded on the meter and from the duration of the test obtained by a stop watch. The rate of flow from the furrow was calculated from the chart on the water level recorder for the depth in the 1-foot HS-type flume.

The depth of flow was determined by a point gage measurement at 12, 18, and 24 feet from the upstream end of the furrow. At the end of each test, the temperature of the water was recorded.

The same procedure was used with furrows constructed in soil, with the exception that the soil was saturated the day before the tests. For the infiltration tests, the vacuum system was operated two hours before the start of the test at 27 inches of mercury and kept in operation throughout the test. During the test period, the infiltration water from each line of ceramic tubes was collected in a 5-gallon jug and measured. The water collected from the five lines of ceramic tubes was divided by the interval of time to obtain the infiltration rate for the test.

RESULTS AND DISCUSSION

Physical Tests

The particle-size distribution significantly affects the infiltration rate of a soil. For example, a small increase in the percentage of dispersed clay or fine silt will usually decrease the infiltration rate.

The results of the mechanical analysis of the soil were clay, 17 percent; fine silt, 25.5 percent; coarse silt, 41.2 percent; and sand, 16.3 percent.

The ease with which soil aggregates are dispersed in water is a measure of soil stability. If the aggregates are relatively stable, the infiltration rate is generally higher and the infiltration rate will remain relatively high. If the aggregates disperse quickly, the infiltration may change rapidly. Knox silt loam was selected as the test soil because of its high structural stability. The infiltration rate remained fairly constant throughout the test, as shown in the appendix.

Hydraulic Measurements

The hydraulic measurements made during the tests were rate of flow (Q), velocity (V), depth (D), and temperature of water (T). Data for all tests are summarized in the Appendix. The velocities were calculated by using the equation $Q = AV$, where A is the area and V is the velocity. The maximum depths determined at points 12, 18, and 24 feet from the upstream end of the furrow were averaged. The water temperature in the supply tank was measured to the nearest 0.1 degree centigrade before and after each test, with a Celsius thermometer.

Calculations of roughness coefficient: The roughness coefficient was determined by using Manning's formula. The roughness coefficient calculated for each test is given in the appendix.

The values of the roughness coefficient were higher for the trapezoidal furrow than for the triangular furrow with the same roughness and the same rate of flow.

The roughness coefficient was plotted versus depth for trapezoidal and triangular furrows. The roughness coefficient decreased with an increase in depth. Figures 4 and 5 show the relationship of roughness coefficient to the depth for three degrees of roughness.

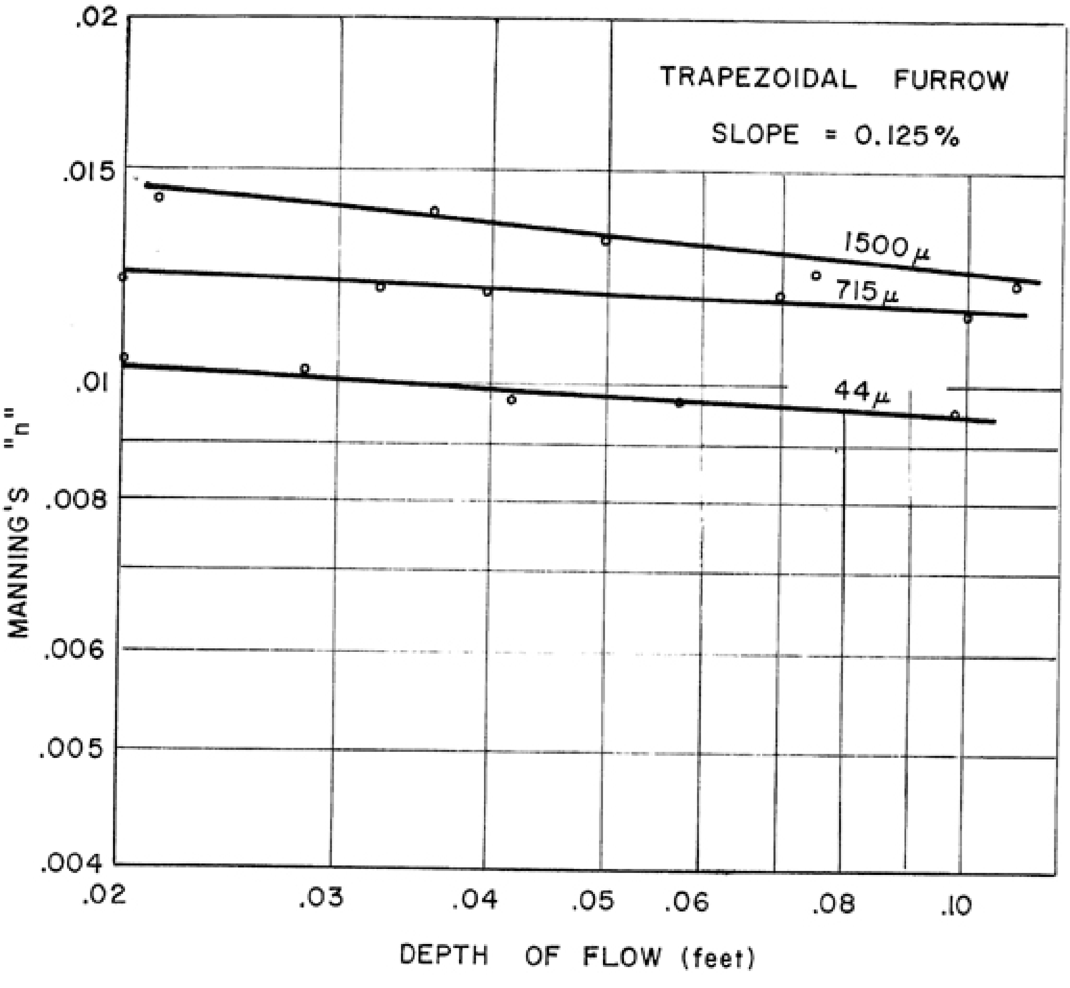

Fig. 4-Variation of roughness coefficient with depth of flow for a trapezoidal furrow.

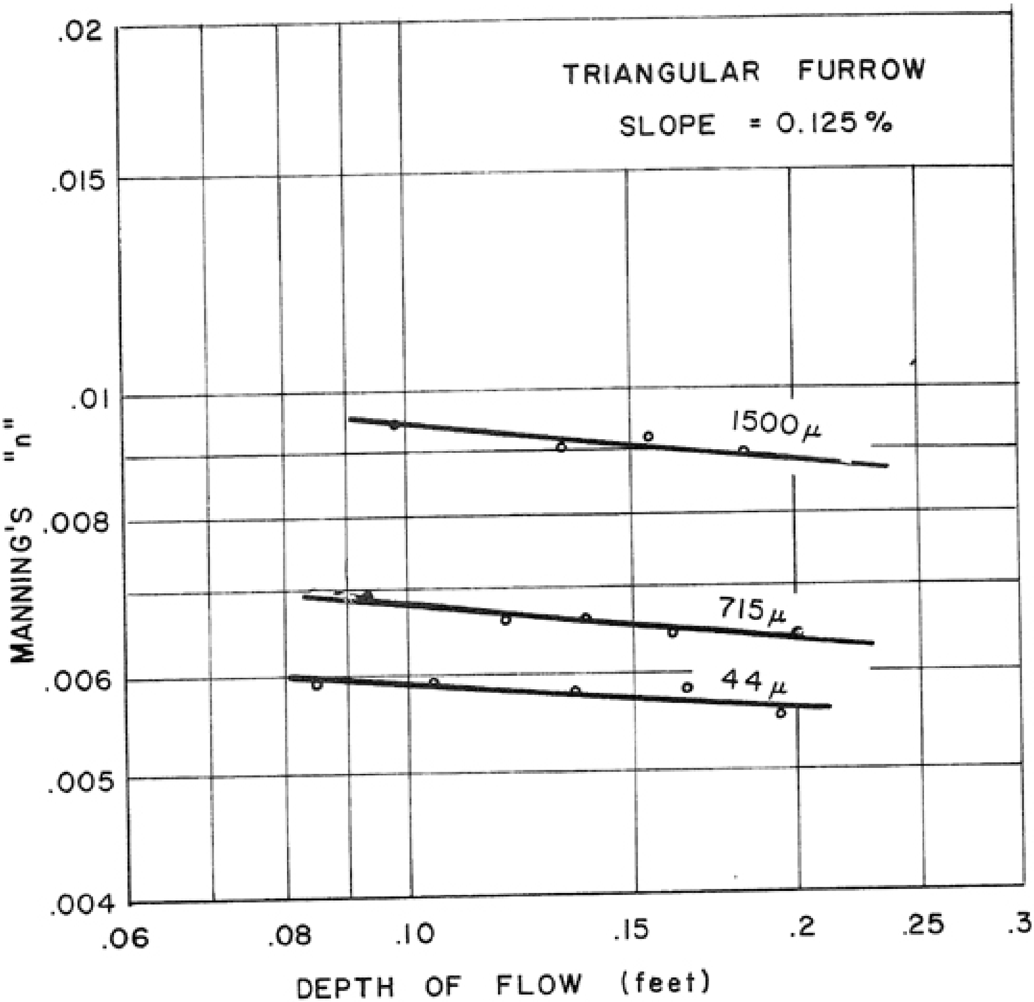

Fig. 5-Variation of roughness coefficient with depth of flow for a triangular furrow.

The relationship between the depth and rate of flow for a triangular furrow with a slope of 0.5 percent and different roughnesses is shown in Figure 6. The triangular furrow was used because of the wider ranges of depths. The depth increased with an increase in rate of flow, and with an increase in the roughness.

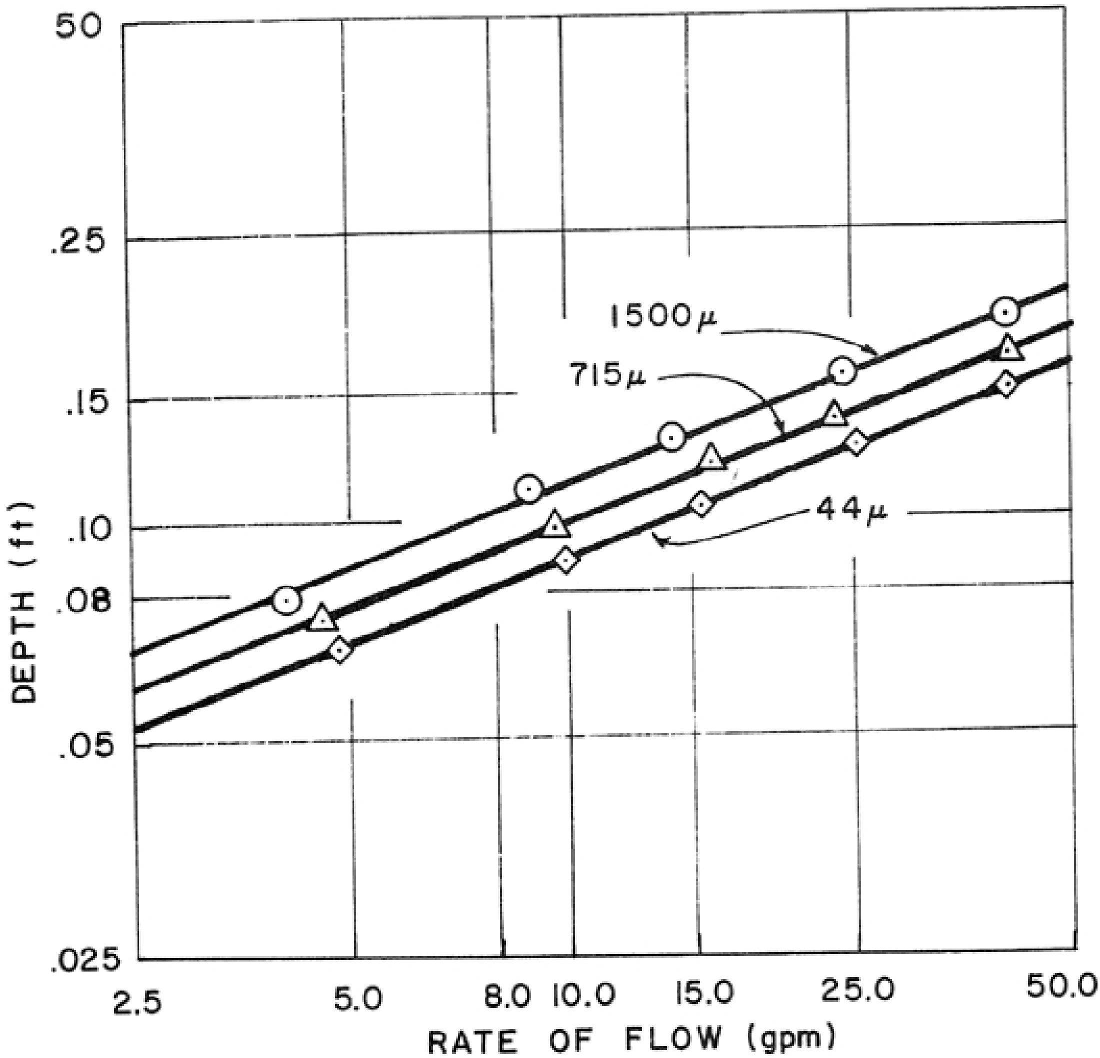

Fig. 6-Relationship of depth to rate of flow for a triangular furrow with a constant slope and different roughnesses.

The relationship between the depth and rate of flow for a triangular furrow with a roughness of 1500 microns and different slopes is shown in Figure 7. The depth increased with an increase in rate of flow, and with a decrease in slope.

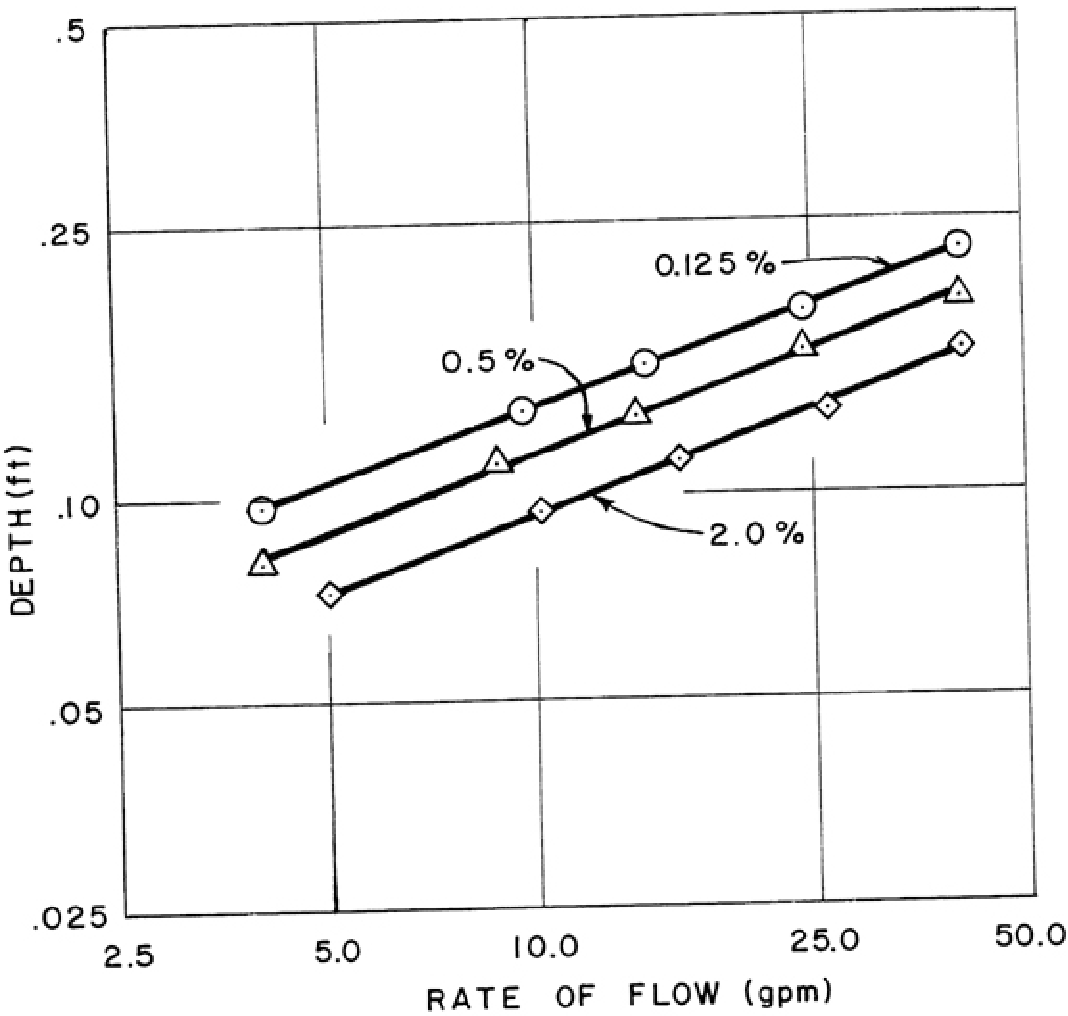

Fig. 7-Relationship of depth to rate of flow for a triangular furrow with a constant roughness and different slopes.

The relationship between the depth and slope of a triangular furrow with a rate of flow of 40 gpm and different roughnesses is shown in Figure 8. The depth decreased with an increase in slope, and with a reduction in roughness.

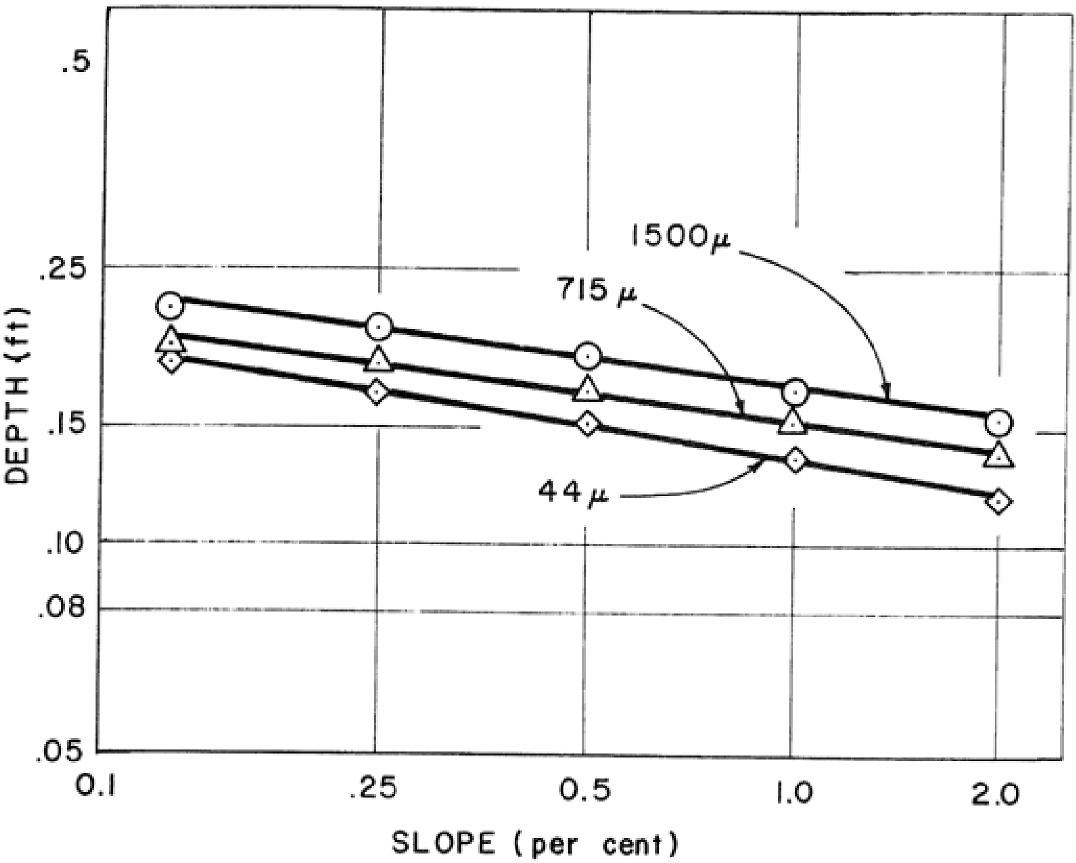

Fig.8-Relationship of depth to slope for a triangular furrow with a constant rate of flow and different roughnesses.

The roughness coefficient was plotted versus velocity for the trapezoidal and traingular furrows. The roughness coefficient decreased with an increase in velocity. Figures 9 and 10 show the relationship of the roughness coefficient to the velocity for the three degrees of roughness.

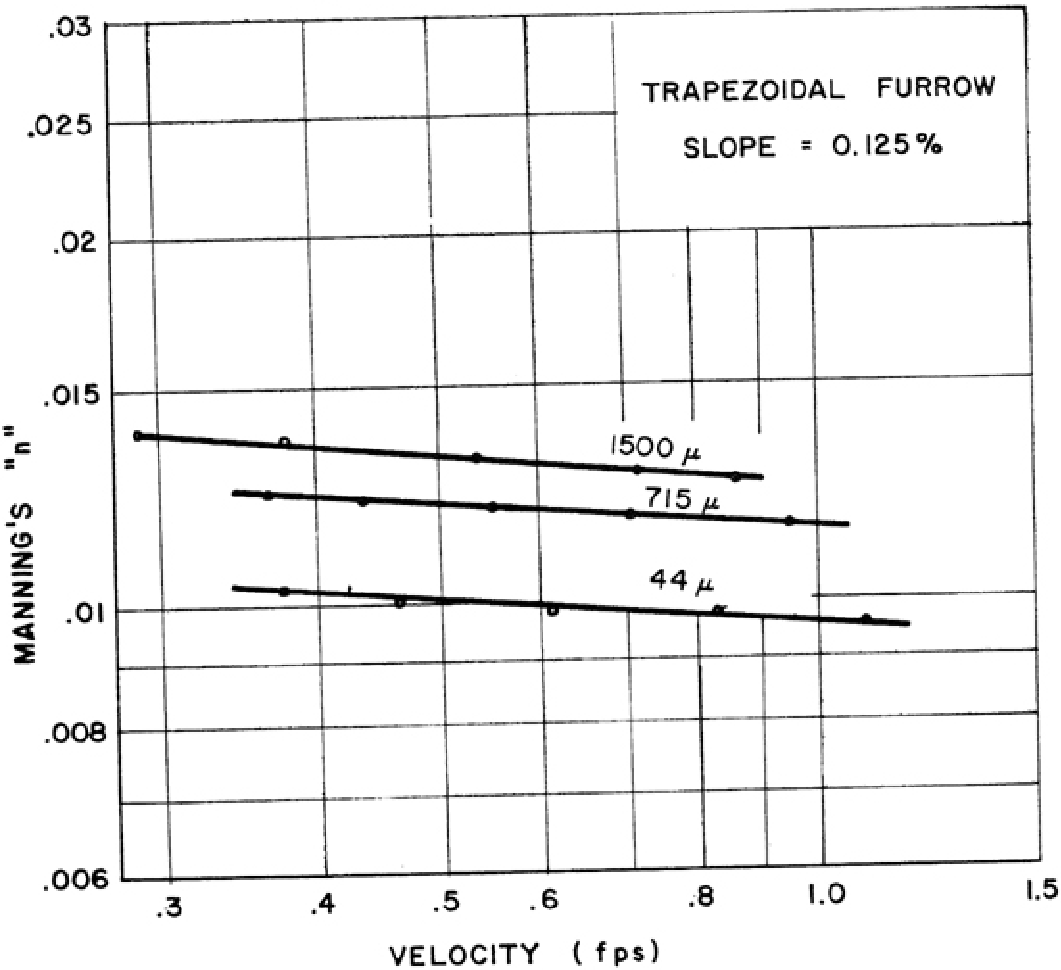

Fig. 9-Relation between roughness coefficient and velocity for a trapezoidal furrow.

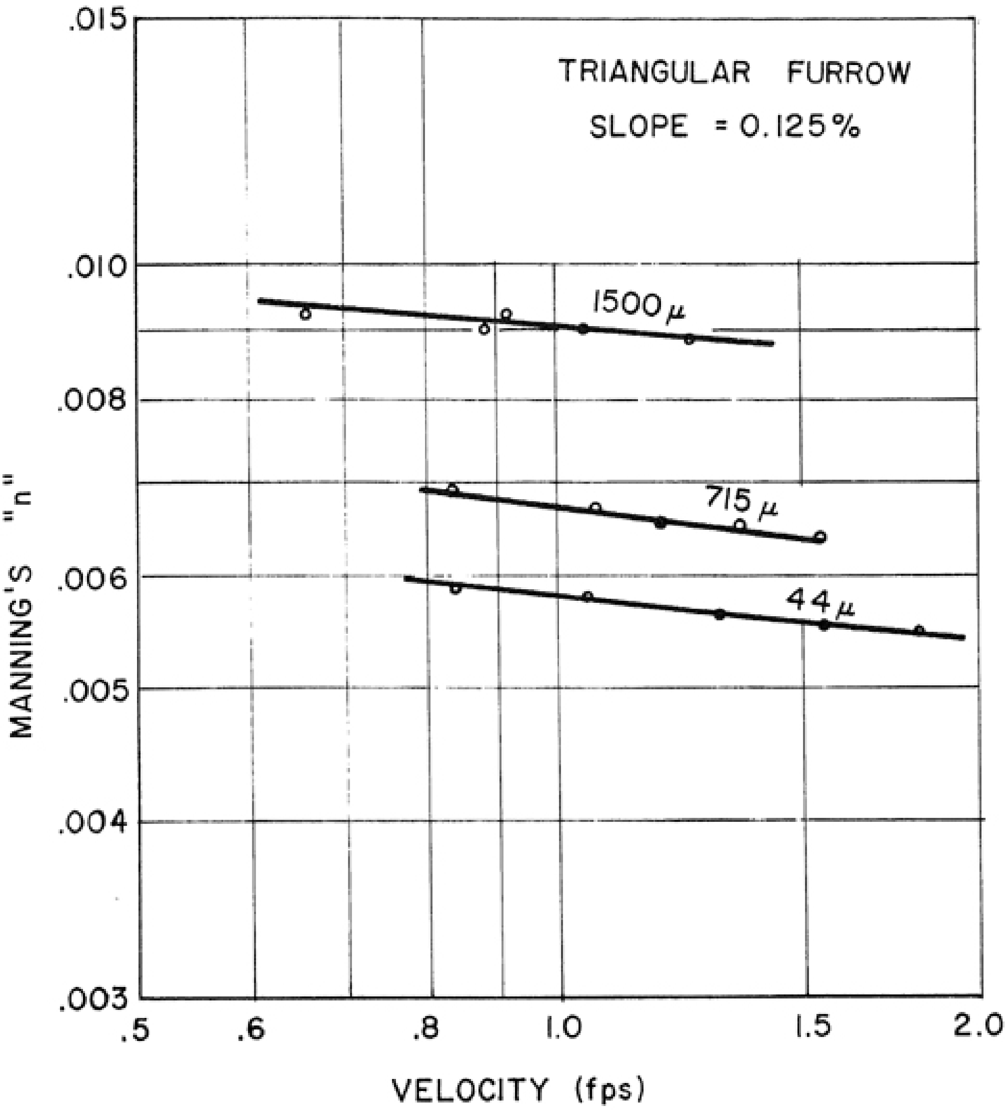

Fig. 10-Relation between roughness coefficient and velocity for a triangular furrow.

The roughness coefficient was plotted versus Reynolds number for the trapezoidal and triangular furrows. Figures 11 and 12 show that for the three degrees of retardance the roughness coefficient decreased with an increase in Reynolds number.

The Reynolds numbers calculated for each test are given in the Appendix. The Reynolds numbers for the triangular furrow ranged from three to eight times those for the trapezoidal furrow. If a Reynolds number of 500 is considered to result in turbulent flow in an open channel, almost all the tests run in the furrows were with turbulent flow.

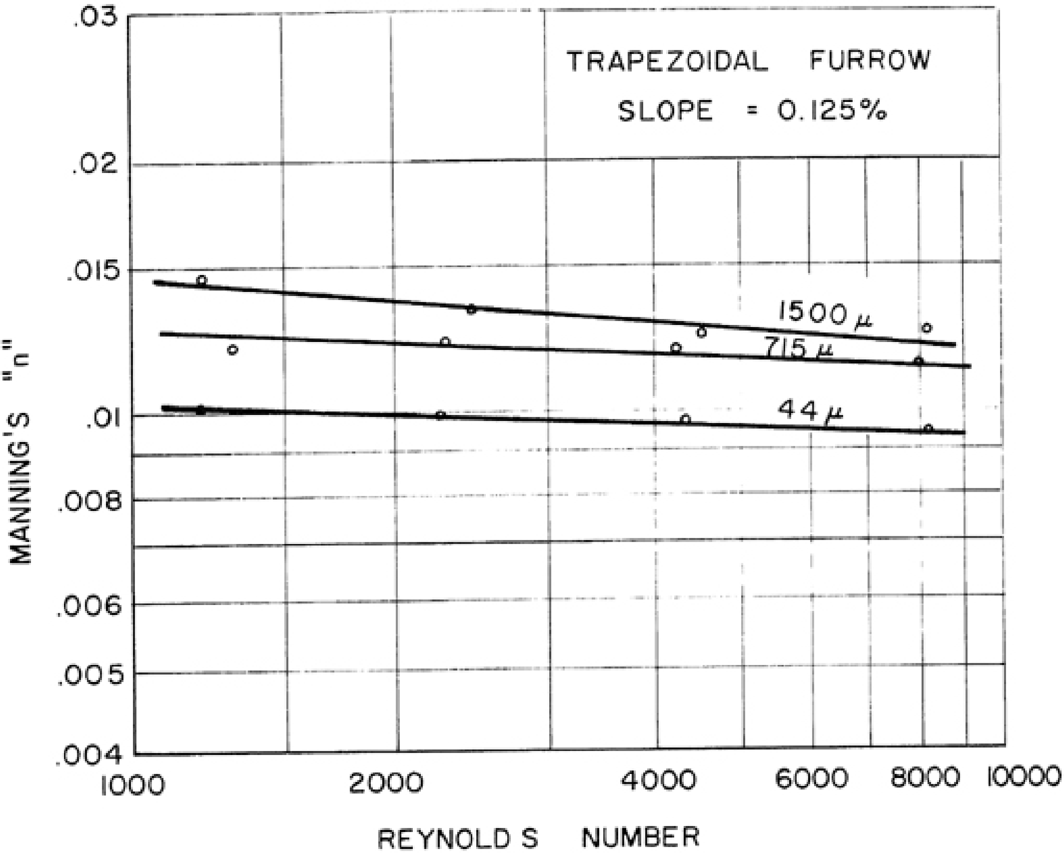

Fig. 11-Variation of roughness coefficient with Reynolds number for a trapezoidal furrow.

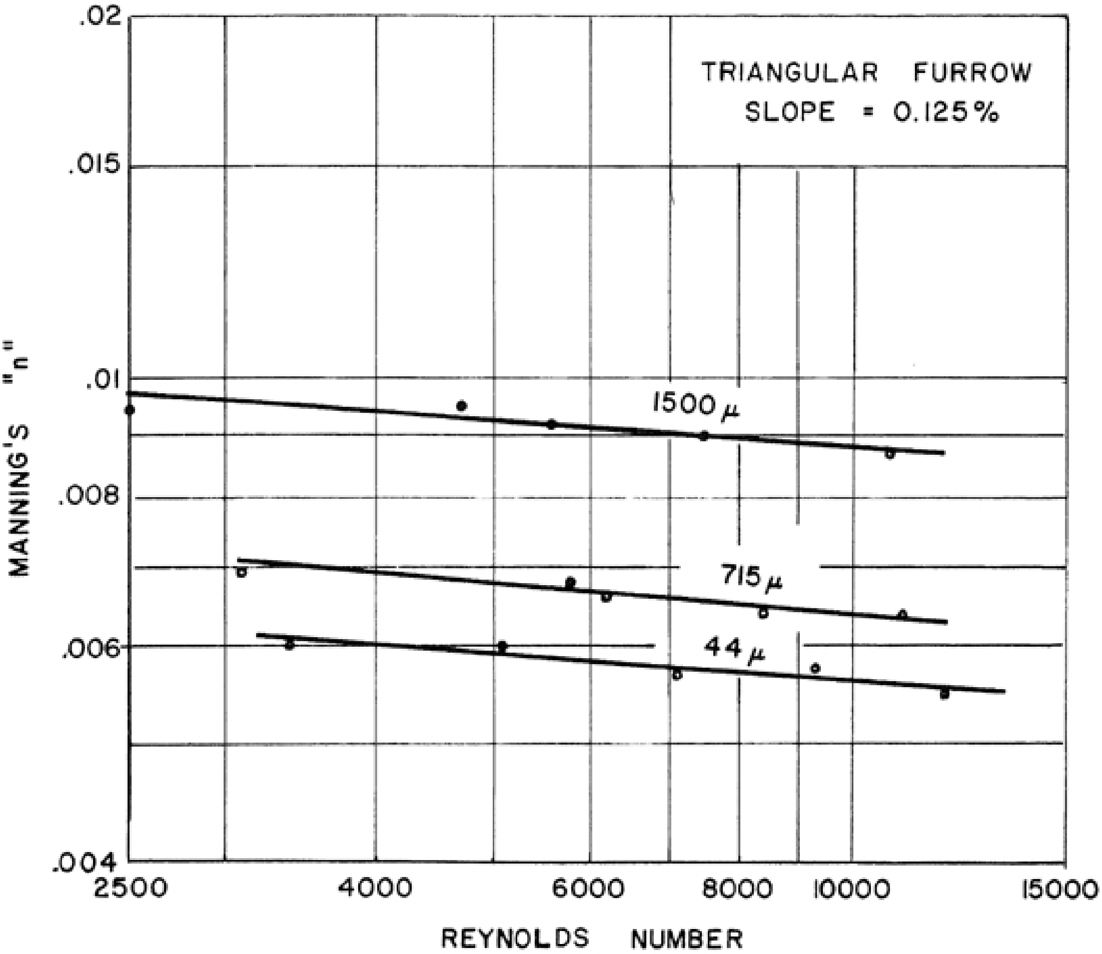

Fig. 12-Variation of roughness coefficient with Reynolds number for a triangular furrow.

The roughness coefficient was plotted versus slope for Reynolds numbers of 1,000 and 5,000 for a trapezoidal furrow and 5,000 and 10,000 for a triangular furrow, as shown in Figures 13 and 14. The ratio of the Reynolds numbers was 1 to 5 for the trapezoidal furrow and 1 to 2 for the triangular furrow, demonstrating that slope affects the roughness coefficient more in the triangular furrow than in the trapezoidal furrow.

The friction factor was plotted versus Reynolds number for the trapezoidal and triangular furrows, as shown in Figures 15 and 16. The friction factor decreased with an increase in Reynolds number.

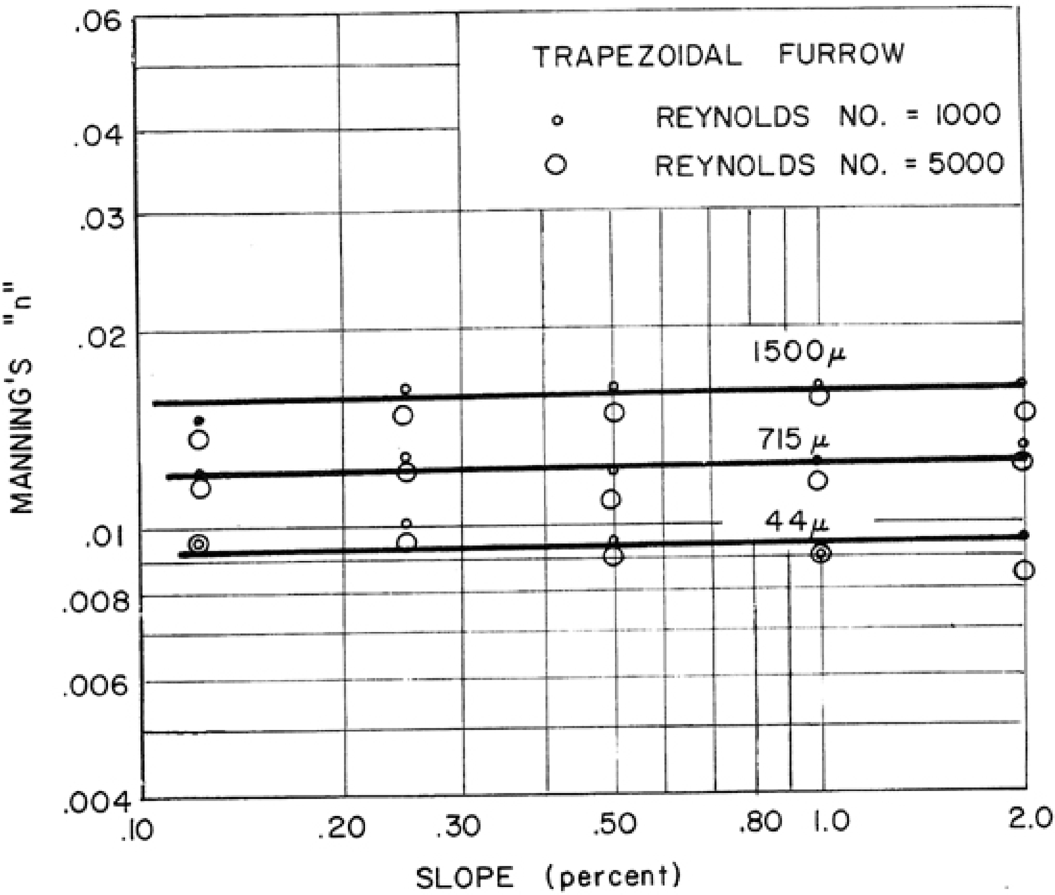

Fig. 13-Relationship of the roughness coefficient to slope for a trapezoidal furrow, with the Reynolds number held constant at two different values.

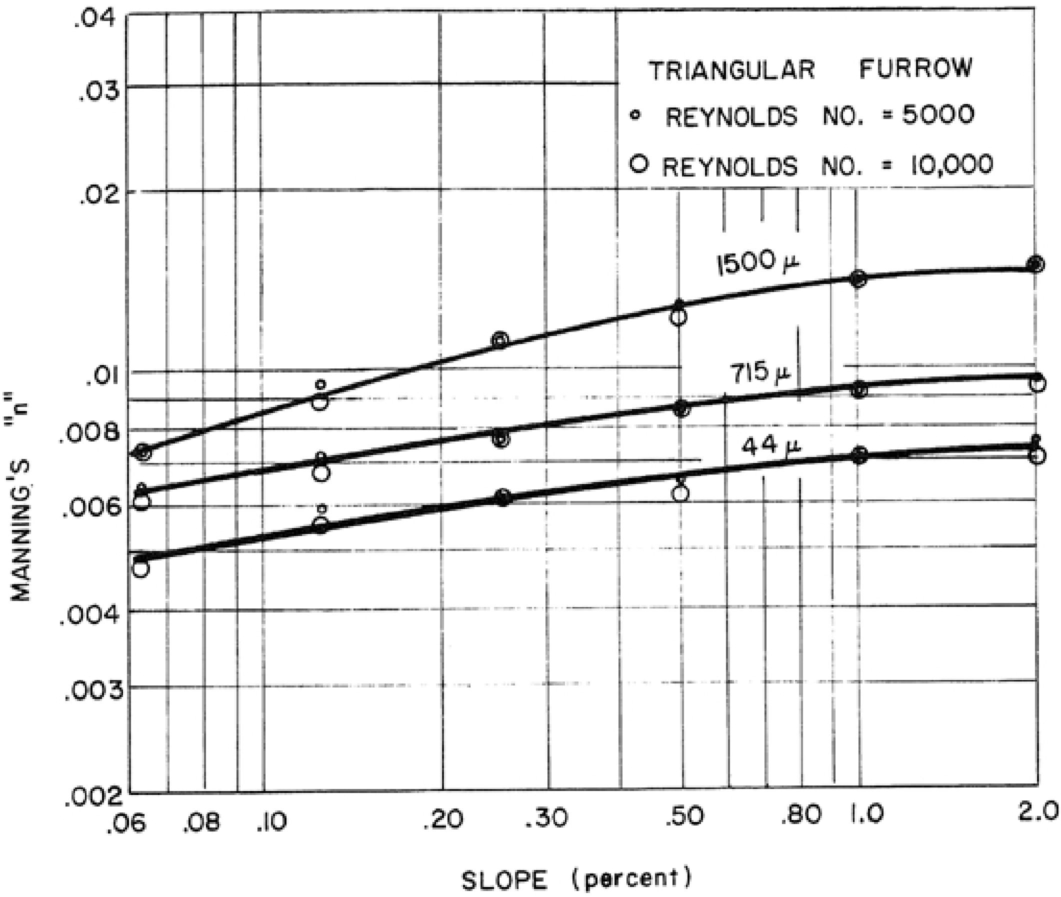

Fig. 14-Relationship of the roughness coefficient to the slope for the triangular furrow with the Reynolds number held constant at two different values.

The friction factor for a selected condition was calculated by using $f = RS/(V^2/2g)$, where R is the hydraulic radius, S is the slope of energy gradient, and $V^2/2g$ is the velocity.

The values of the friction factor were higher for the trapezoidal furrow than for the triangular furrow with the same roughness.

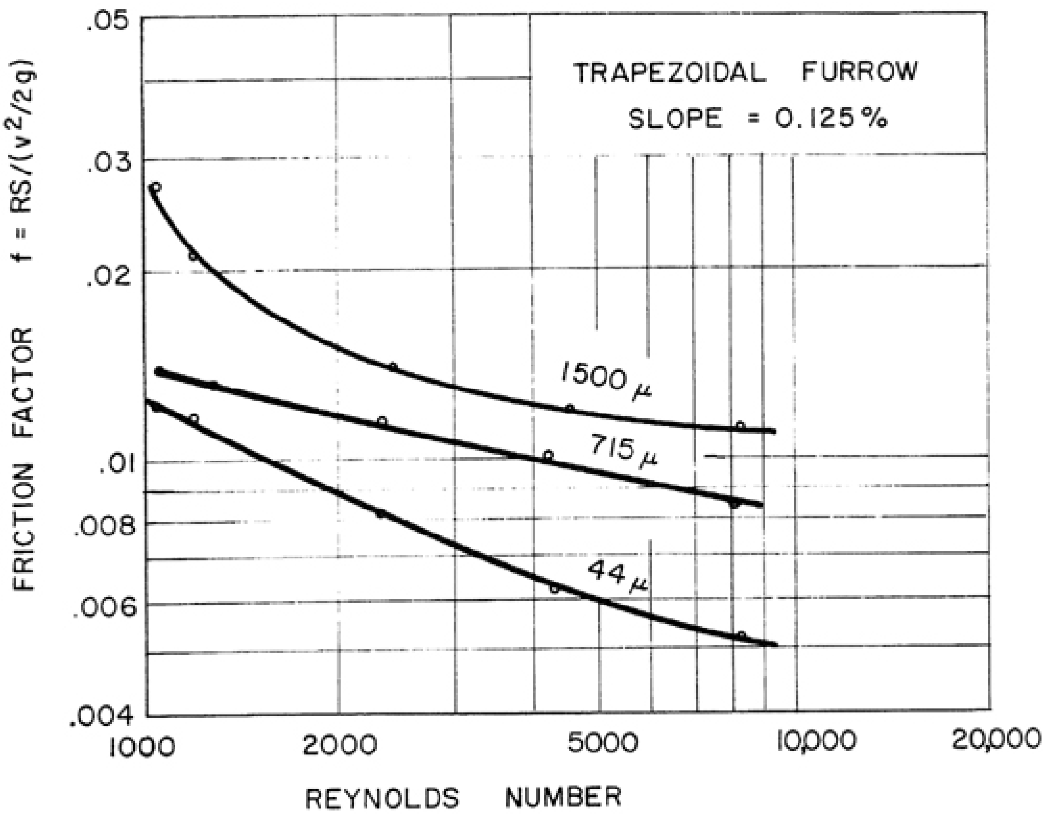

Fig. 15-Relationship of the friction factor to the Reynolds number for a trapezoidal furrow.

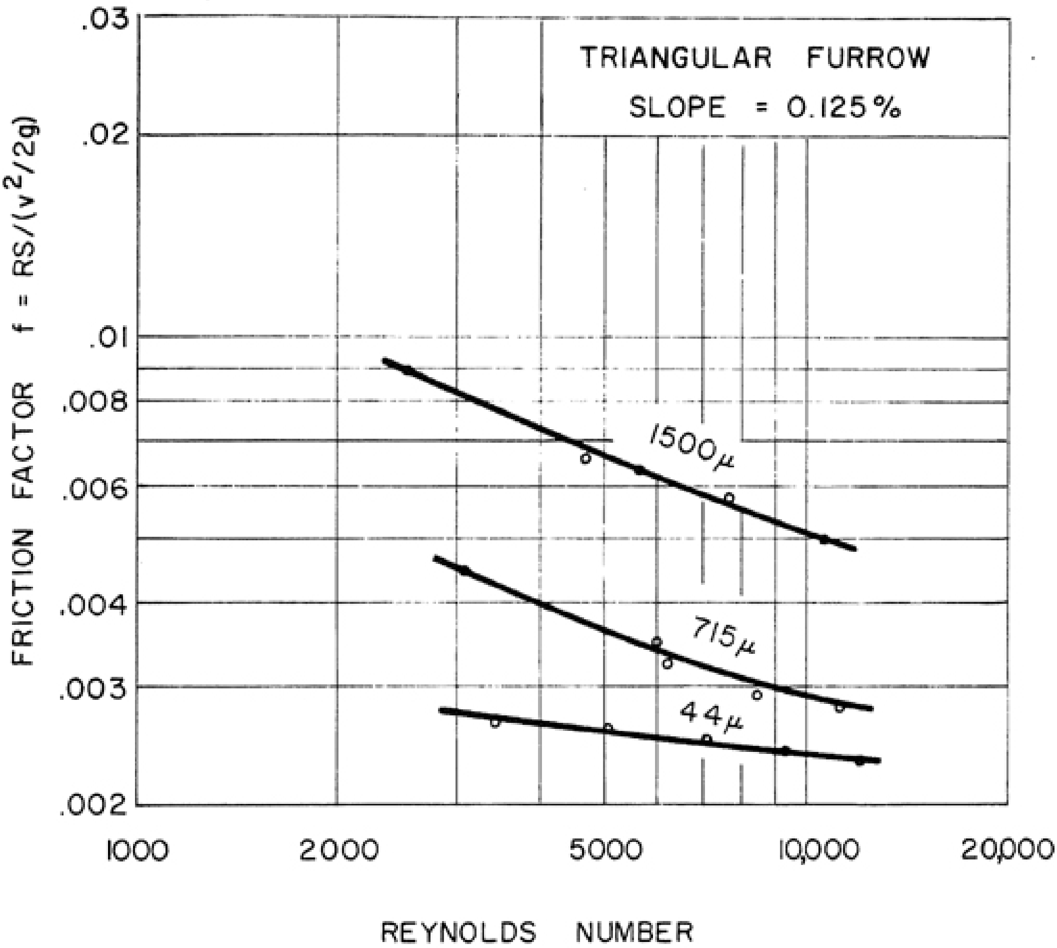

Fig.16-Relationship of the friction factor to the Reynolds number for a triangular furrow.

Calculation of Froude number: The Froude number was calculated to determine the state of flow in the furrows. These values are given in the Appendix. At a Froude number of unity, the flow is said to be in a critical state. If the Froude number is less than unity, the flow is subcritical; if greater than unity, the flow is supercritical.

Effect of furrow shape on infiltration: The infiltration rates were calculated by using the volume of water removed from the soil, divided by the area of the water surface in the furrow and the time. The volume used was the total water obtained in the five jugs.

The individual infiltration rates ranged from 0.09 to 0.14 inch per hour for the trapezoidal furrow, with the average being 0.12 inch per hour. The individual infiltration rates ranged from 0.8 to 1.4 inches per hour for the triangular furrow, with the average being 0.87 inch per hour.

The differences in infiltration rates in the two furrows can be explained by the differences in depth of flow, deposition of sediment, and the ratio of wetted perimeter to width of water surface.

The effective head on the saturated zone increases with depth of flow. As the depth of water increases, the saturated zone under a furrow occupies an increasingly larger fraction of the total wetted profile, and the moisture gradients in the unsaturated part of the profile become relatively steeper. For the same rate of flow, the maximum depth of water in the triangular furrow was about five times the depth of that in the trapezoidal furrow. With the surface of the furrow saturated, the differences in depths of water would account for part of the differences in the infiltration rates of the two furrow shapes.

A volume of slowly permeable sediment coming from a suspension of silt and clay would affect a relatively larger percent of the wetted perimeter of the trapezoidal furrow than would be true with the triangular furrow. Therefore, the infiltration rate for the trapezoidal furrow should be less than the rate for the triangular furrow.

The ratio of wetted perimeter to width of water surface was 1.02 for the trapezoidal furrow and 1.20 for the triangular furrow. This also would help explain a higher infiltration rate in the triangular furrow.

Scatter in Data

There was considerable scatter in the graphic representation of the data presented. A factor is given which may help to explain this scatter.

Depth measurements. At shallow flows, the resistance of the sides of the furrow to wetting affected the water surface and thereby affected the depth measurements in some tests. There were slight rapid fluctuations on the water surface tension. In these cases, judgment of the observer was an important factor. Even in the calculated velocity, there was the error caused by the side effects on water surface and the accuracy of the depth measurements.

CONCLUSIONS

Results of this investigation suggest the following conclusions:

1. The roughness coefficient was a function of the depth, velocity, and Reynolds number. The roughness coefficient decreased with an increase in each of these four variables.
2. The values of roughness coefficient were higher for the trapezoidal furrow than for the triangular furrow with the same rate of flow, degree of roughness, and slope.
3. The Reynolds numbers for the triangular furrow ranged from three to eight times those for the trapezoidal furrow with the same rate of flow, degree of roughness, and slope.
4. The individual infiltration rates ranged from 0.09 to 0.14 inch per hour with the average being 0.12 inch per hour for the trapezoidal furrow. The individual infiltration rate ranged from 0.8 to 1.4 inches per hour with an average being 0.87 inch per hour for the triangular furrow. Most of the differences in infiltration rates for the two furrow shapes can be attributed to the differences in depth of flow, deposition of sediment, and ratio of wetted perimeter to width of water surface.

REFERENCES

1. American Society for Testing Materials, Committee D-18, Procedures for Testing Soils, Philadelphia, Pennsylvania: American Society for Testing Materials, July 1950.
2. Harrold, L. L., and D. B. Krimgold, "Devices for Measuring Rates and Amounts of Runoff", SCS-TP-51, July 1943. Revised October 1944.
3. Horton, R. E., H. R. Leach, and R. Van Vliet, "Laminar Sheet Flow", Transactions American Geophysical Union, Part 2, pp. 393-404, June 1934.
4. King, Horace Williams, Handbook of Hydraulics, Fourth Edition; New York: McGraw-Hill Book Company, Inc., 1954.
5. Owen, W. M., "Laminar to Turbulent Flow in a Wide Open Channel", Transactions American Society of Civil Engineering, 119:1157-1175, 1954.
6. Parsons, D.A., "Depths of Overland Flow", (SCS-TP-82, July 1949.
7. Powell, R. W., "Resistance to Flow in Rough Channels", Transactions American Geophysical Union, August 1950, 31:575-582.
8. Rouse, Hunter, and Simon Ince, History of Hydraulics, Iowa City, Iowa: Iowa Institute of Hydraulic Research 1957.

APPENDIX

Summary of Original Data

The original data recorded during the experiment and the values of the Reynolds number, Froude number, and Manning's n are summarized in the following tables.

TABLE 1 - SUMMARY OF DATA FOR TRAPEZOIDAL FURROW WITH DIFFERENT ROUGHNESSES

Test No.	Temp. C°	Slope %	Rate of flow gpm	Velocity fps	Depth ft.	Reynolds number	Froude number	Manning's n
				Smooth Aluminum Surface				
1	20.0	2.0	80.2	3.00	0.034	9230	2.970	0.0070
2	20.0		38.9	2.30	0.022	4593	2.779	0.0070
3	20.0		18.0	1.56	0.015	2157	2.295	0.0080
4	20.0		9.3	1.20	0.010	1129	2.182	0.0078
5	20.0		6.0	1.10	0.007	737	2.448	0.0076
6	20.0	1.0	79.8	2.04	0.050	8905	1.644	0.0095
7	20.0		39.3	1.50	0.034	4527	1.457	0.0101
8	20.0		18.3	1.09	0.022	2155	1.305	0.0105
9	20.0		9.4	0.85	0.014	1132	1.329	0.0097
10	20.0		5.6	0.83	0.009	682	1.245	0.0097
11	20.0	0.5	79.8	1.75	0.059	8934	1.298	0.0087
12	20.0		39.3	1.30	0.039	4434	1.184	0.0090
13	20.0		18.4	0.96	0.025	2155	1.083	0.0092
14	20.0		8.8	0.73	0.016	1062	1.025	0.0091
15	20.0		6.3	0.70	0.012	762	1.020	0.0088
16	20.0	0.25	80.8	1.29	0.078	8541	0.842	0.0098
17	20.0		39.8	0.96	0.053	4417	0.750	0.0104
18	20.0		18.3	0.68	0.037	2094	0.596	0.0106
19	20.0		8.8	0.50	0.025	1035	0.520	0.0105
20	20.0		6.4	0.47	0.018	769	0.625	0.0107
21	20.0	0.125	80.8	1.10	0.091	8341	0.664	0.0091
22	20.0		39.8	0.87	0.058	4379	0.653	0.0086
23	20.0		18.2	0.60	0.039	2066	0.545	0.0097
24	20.0		9.4	0.44	0.028	1101	0.468	0.0097
25	20.0		5.8	0.38	0.020	687	0.480	0.0099
26	20.0	2.0	78.2	2.96	0.034	9004	2.898	0.0071
27	20.0		39.3	2.30	0.023	4645	2.632	0.0074
28	20.0		18.2	1.60	0.015	2204	2.992	0.0074
29	20.0		8.3	1.14	0.009	1100	2.354	0.0077
30	20.0		5.6	1.10	0.006	687	2.817	0.0076
				44-Micron Silt Surface				
31	20.0	2.0	80.2	2.80	0.037	9190	2.615	0.0081
32	20.0		39.8	1.98	0.026	4610	2.172	0.0091
33	20.0		18.8	1.38	0.018	2244	1.824	0.0104
34	20.0		9.9	0.90	0.015	1189	1.266	0.0104
35	20.0		6.1	0.78	0.011	735	1.241	0.0100

TABLE 1 (CONTINUED)

Test No.	Temp. C°	Slope %	Rate of flow gpm	Velo-city fps	Depth ft.	Reynolds number	Froude number	Manning's n
36	20.0	2.0	80.5	2.82	0.037	9226	2.625	0.0081
37	20.0		41.8	2.24	0.024	4905	2.614	0.0085
38	20.0		21.1	1.40	0.015	2534	2.497	0.0087
39	20.0		10.4	1.04	0.012	1249	1.448	0.0096
40	20.0		4.7	0.70	0.008	573	1.254	0.0097
41	20.0	1.0	81.5	2.04	0.051	9075	1.629	0.0096
42	20.0		41.2	1.62	0.033	4745	1.598	0.0091
43	20.0	1.0	19.4	1.16	0.022	2288	1.485	0.0099
44	20.0		9.9	0.94	0.014	1196	1.404	0.0092
45	20.0		6.1	0.80	0.010	742	1.435	0.0094
46	20.0	0.5	82.6	1.72	0.061	9030	1.258	0.0091
47	20.0		40.7	1.35	0.039	4643	1.225	0.0087
48	20.0		19.4	0.94	0.027	2264	1.016	0.0099
49	20.0		10.8	0.74	0.019	1283	0.960	0.0099
50	20.0		7.1	0.62	0.015	850	0.905	0.0101
51	20.0	0.25	82.3	1.28	0.080	8684	0.826	0.0101
52	20.0		40.5	1.02	0.052	4511	0.810	0.0097
53	20.2		19.4	0.72	0.035	2233	0.685	0.0100
54	20.2		10.5	0.56	0.025	1225	0.616	0.0104
55	20.2		6.1	0.44	0.019	721	0.540	0.0104
56	20.0	0.125	79.5	1.10	0.087	8280	0.700	0.0096
57	20.0		40.5	0.84	0.059	4361	0.645	0.0098
58	20.0		20.2	0.62	0.042	2296	0.543	0.0099
59	20.0		10.5	0.47	0.029	1218	0.492	0.0103
60	19.8		5.8	0.38	0.020	681	0.480	0.0103
			715-Micron Sand Surface					
61	18.9	2.0	83.2	2.13	0.050	9038	1.715	0.0128
62	19.0		42.6	1.68	0.033	4768	1.650	0.0125
63	19.0		20.8	1.24	0.022	2386	1.520	0.0131
64	19.1		10.9	0.96	0.015	1273	1.386	0.0132
65	19.1		5.7	0.76	0.010	677	1.339	0.0127
66	18.9	1.0	83.0	1.85	0.057	8897	1.401	0.0113
67	21.0		41.8	1.38	0.039	4850	1.256	0.0119
68	21.0		20.2	1.06	0.025	2417	1.192	0.0117
69	20.4		11.0	0.80	0.018	1315	1.060	0.0126
70	20.2		6.2	0.69	0.012	651	1.111	0.0122
71	21.8	0.50	84.2	1.54	0.069	9416	1.059	0.0111
72	18.9		42.8	1.17	0.047	4674	0.967	0.0114
73	19.8		21.1	0.86	0.032	2424	0.858	0.0120
74	20.0		10.5	0.63	0.022	1240	0.751	0.0129
75	20.2		5.8	0.53	0.013	690	0.717	0.0128
76	21.8	0.25	84.2	1.12	0.093	9000	0.670	0.0127
77	21.8		42.0	0.87	0.061	4767	0.639	0.0126
78	20.8		21.0	0.66	0.041	2434	0.584	0.0130
79	22.8		10.6	0.43	0.031	1299	0.581	0.0128
80	20.8		5.5	0.45	0.017	668	0.549	0.0131

TABLE 1 (CONTINUED)

Test No.	Temp. C°	Slope %	Rate of flow gpm	Velocity fps	Depth ft.	Reynolds number	Froude number	Manning's n
81	18.4	0.125	83.0	0.95	0.107	8032	0.531	0.0116
82	19.1		42.2	0.72	0.071	4244	0.487	0.0119
83	19.1		21.3	0.56	0.049	2334	0.465	0.0121
84	22.8		10.6	0.42	0.033	1298	0.453	0.0120
85	21.2		5.6	0.33	0.020	685	0.409	0.0123
1500-Micron Sand Surface								
86	15.0	2.0	83.2	1.93	0.055	8594	1.483	0.0151
87	16.0		42.2	1.52	0.036	4541	1.434	0.0146
88	17.0		21.6	1.07	0.026	2331	1.180	0.0168
89	18.0		10.5	0.81	0.017	1209	1.119	0.0166
90	18.0		5.4	0.58	0.013	615	0.846	0.0161
91	18.3	1.0	83.9	1.56	0.067	8402	1.105	0.0148
92	18.2		42.2	1.18	0.046	4545	0.985	0.0156
93	18.1		21.0	0.85	0.032	2322	0.852	0.0171
94	18.0		10.8	0.59	0.025	1205	0.688	0.0161
95	18.0		6.0	0.50	0.016	682	0.634	0.0163
96	18.4	0.5	83.2	1.22	0.085	8392	0.761	0.0156
97	18.5		42.6	0.99	0.055	4538	0.758	0.0148
98	18.7		21.4	0.71	0.039	2368	0.645	0.0164
99	19.0		11.0	0.50	0.029	1246	0.517	0.0165
100	21.5		4.8	0.36	0.018	588	0.465	0.0164
101	20.0	0.25	83.6	1.06	0.097	8550	0.623	0.0158
102	20.5		42.6	0.81	0.066	4650	0.573	0.0161
103	20.5		21.3	0.58	0.047	2416	0.482	0.0161
104	20.1		11.0	0.43	0.033	1266	0.427	0:0172
105	21.0		5.6	0.35	0.021	682	0.433	0.0167
106	20.0	0.125	83.6	0.85	0.110	8360	0.563	0.0120
107	19.9		42.8	0.70	0.075	4533	0.475	0.0124
108	19.9	0.125	22.0	0.50	0.052	2433	0.427	0.0131
109	19.8		10.6	0.38	0.036	1209	0.361	0.0146
110	19.9		5.1	0.29	0.023	602	0.343	0.0148

Knox Silt Loam with Infiltration

Test No.	Temp. C°	Slope %	Rate of flow gpm	Velocity fps	Depth ft.	Infiltration rate in./hr.	Reynolds number	Froude number	Manning's n
111	20.5	1.0	10.1	0.95	0.020	0.09	1233	1.560	0.0147
112	20.0		7.3	0.79	0.012	0.09	944	1.274	0.0146
113	19.5		5.8	0.66		0.10	659	1.112	0.0156
114	19.0		3.9	0.58	0.009	0.10	550	1.042	0.0163
115	19.0		1.9	0.30	0.008	0.10	245	0.506	0.0163
116	19.0	1.0	9.6	0.74	0.016	0.09	980	1.038	0.0160
117	19.0		6.7	0.54	0.014	0.10	810	0.859	0.0163
118	19.0		5.0	0.52	0.013	0.09	593	0.831	0.0159
119	21.0		3.1	0.36	0.011	0.10	395	0.791	0.0164
120	21.0		1.8	0.29	0.009	0.09	210	0.686	0.0152

TABLE 1 (CONTINUED)

Test No.	Temp. C°	Slope %	Rate of flow gpm	Velocity fps	Depth ft.	Infiltration rate in./hr.	Reynolds number	Froude number	Manning's n
121	19.0	0.50	8.3	0.58	0.018	0.09	836	0.783	0.0120
122	19.0		5.6	0.50	0.013	0.09	581	0.786	0.0130
123	19.0		4.6	0.47	0.012	0.09	557	0.781	0.0128
124	19.0		2.1	0.28	0.010	0.09	219	0.636	0.0131
125	19.0		0.7	0.15	0.009	0.09	109	0.585	0.0136
126	19.0	0.25	15.4	0.56	0.031	0.10	1438	0.578	0.0120
127	19.0		10.1	0.50	0.024	0.10	977	0.582	0.0126
128	19.0		5.6	0.43	0.016	0.08	547	0.617	0.0123
129	19.0		4.4	0.38	0.014	0.08	484	0.584	0.0120
130	19.0		2.2	0.19	0.013	0.09	154	0.560	0.0130
131	20.0	0.125	31.3	0.59	0.058	0.11	2879	0.747	0.0124
132	20.0		24.4	0.54	0.049	0.10	2454	0.484	0.0121
133	20.0		19.6	0.53	0.044	0.11	1992	0.460	0.0124
134	20.0		7.4	0.35	0.025	0.11	753	0.393	0.0124
135	20.0		4.2	0.26	0.019	0.10	352	0.334	0.0128
136	22.0	0.0625	36.8	0.55	0.071	0.13	3534	0.384	0.0116
137	21.0		27.7	0.51	0.062	0.14	2729	0.375	0.0115
138	21.0		21.3	0.47	0.054	0.13	2274	0.369	0.0117
139	21.0		12.8	0.36	0.040	0.14	1346	0.317	0.0122
140	22.0		5.0	0.24	0.025	0.14	548	0.273	0.0125

Knox Silt Loam without Infiltration

Test No.	Temp. C°	Slope %	Rate of flow gpm	Velocity fps	Depth ft.	Reynolds number	Froude number	Manning's n
141	21.0	2.0	15.7	1.16	0.018	1711	1.630	0.0115
142	21.0		12.4	1.07	0.014	1490	1.612	0.0117
143	21.2		7.3	0.90	0.010	768	1.605	0.0120
144	21.2		3.4	0.52	0.008	456	1.068	0.0126
145	21.2		1.8	0.36	0.007	171	1.038	0.0130
146	21.2	1.0	15.4	0.94	0.020	1611	1.310	0.0115
147	21.2		11.8	0.90	0.016	1205	1.286	0.0114
148	21.2		8.0	0.73	0.013	826	1.145	0.0125
149	20.4		4.5	0.60	0.009	453	1.144	0.0116
150	19.0		1.7	0.32	0.007	342	1.120	0.0127
151	19.0	0.50	20.9	0.86	0.030	1997	0.906	0.0122
152	19.0		15.7	0.72	0.027	1420	0.803	0.0129
153	20.2		10.2	0.60	0.020	958	0.785	0.0129
154	20.5		5.2	0.44	0.015	672	0.627	0.0127
155	20.0		2.2	0.32	0.010	338	0.560	0.0126
156	20.0	0.25	26.9	0.71	0.046	2690	0.594	0.0124
157	21.6		21.5	0.66	0.040	2253	0.592	0.0121
158	22.4		14.7	0.56	0.032	1577	0.557	0.0125
159	23.6		8.0	0.44	0.022	871	0.556	0.0122
160	23.6		3.0	0.29	0.013	323	0.423	0.0126
161	23.6	0.125	36.3	0.62	0.064	3686	0.445	0.0128
162	23.6		28.0	0.59	0.056	3072	0.449	0.0124

TABLE 1 (CONTINUED)

Test No.	Temp. C°	Slope %	Rate of flow gpm	Velo-city fps	Depth ft.	Reynolds number	Froude number	Manning's n
163	22.6		20.5	0.52	0.048	2286	0.430	0.0126
164	22.4		13.2	0.41	0.037	1397	0.385	0.0134
165	22.4		8.0	0.36	0.026	771	0.331	0.0130
166	22.0	0.0625	36.1	0.53	0.071	3403	0.369	0.0120
167	22.0		28.1	0.51	0.061	2910	0.392	0.0121
168	22.0		20.9	0.49	0.053	2310	0.374	0.0124
169	22.0		14.2	0.39	0.043	1516	0.331	0.0126
170	22.0		5.5	0.26	0.025	618	0.296	0.0119

TABLE 2 - SUMMARY OF DATA FOR TRIANGULAR FURROW WITH DIFFERENT ROUGHNESSES

Test No.	Temp. C°	Slope %	Rate of flow gpm	Velo-city fps	Depth ft.	Reynolds number	Froude number	Manning's n
				Smooth Aluminum Surface				
171	19.0	2.0	41.2	4.42	0.118	19532	3.204	0.0064
172	19.0		27.6	3.97	0.012	15150	3.094	0.0065
173	19.0		15.5	3.78	0.083	11743	3.271	0.0059
174	19.0		10.2	3.09	0.070	8096	2.410	0.0065
175	19.0		5.0	2.78	0.051	5315	3.071	0.0059
176	18.8	1.0	41.5	3.37	0.135	17049	2.284	0.0065
177	19.8		25.2	2.89	0.114	12581	2.137	0.0067
178	19.8		15.3	2.63	0.093	9329	2.148	0.0065
179	19.4		9.4	2.30	0.078	6775	2.052	0.0066
180	19.2		4.6	2.21	0.056	4640	2.328	0.0068
181	18.3	0.50	41.2	2.67	0.152	14931	1.716	0.0062
182	18.3		28.2	2.16	0.130	11272	1.796	0.0057
183	18.9		12.8	2.01	0.097	7325	1.610	0.0062
184	19.0		10.3	1.93	0.087	6628	1.718	0.0057
185	19.0		4.9	1.72	0.065	4186	1.684	0.0065
186	18.1	0.25	41.2	2.30	0.163	13779	1.418	0.0054
187	18.0		25.0	1.97	0.137	9925	1.325	0.0056
188	17.9		15.4	1.72	0.115	7234	1.262	0.0057
189	17.8		9.3	1.55	0.094	5309	1.258	0.0055
190	17.7		5.2	1.41	0.074	3808	1.292	0.0062
191	16.8	0.125	41.5	1.99	0.175	12456	1.193	0.0056
192	17.0		24.6	1.73	0.145	9026	1.137	0.0057
193	17.0		14.4	1.54	0.117	6526	1.132	0.0055
194	17.1		10.4	1.43	0.103	5320	1.120	0.0055
195	17.7		5.2	1.22	0.079	3592	1.089	0.0054
196	15.5	0.0625	41.5	1.31	0.217	9791	0.702	0.0057
197	15.6		25.0	1.20	0.176	7263	0.713	0.0054
198	15.8		15.9	1.06	0.149	5447	0.687	0.0058
199	16.0		9.8	0.94	0.124	4085	0.667	0.0055
200	16.2		5.4	0.86	0.096	2917	0.694	0.0060
				44-Micron Silt Surface				
201	19.8	2.0	40.4	4.28	0.118	19301	3.109	0.0066
202	19.6		25.0	3.56	0.102	13869	2.781	0.0072
203	19.5		16.3	3.28	0.081	10082	2.871	0.0067
204	21.6		9.8	2.87	0.071	8131	2.681	0.0070
205	22.2		5.0	2.66	0.053	5692	2.885	0.0071
206	20.0	1.0	40.7	3.19	0.138	16947	2.140	0.0069
207	20.0		24.6	2.78	0.115	12295	2.043	0.0071
208	20.0		16.2	2.56	0.097	9568	2.046	0.0068
209	20.1		10.1	2.34	0.080	7226	2.067	0.0066
210	20.0		5.6	2.17	0.062	5179	2.170	0.0070
211	20.0	0.50	40.5	2.55	0.153	15041	1.628	0.0066
212	20.0		25.2	2.29	0.128	11278	1.596	0.0065
213	20.1	0.50	15.2	2.04	0.105	8268	1.572	0.0064

TABLE 2 (CONTINUED)

Test No.	Temp. C°	Slope %	Rate of flow gpm	Velo-city fps	Depth ft.	Reynolds number	Froude number	Manning's n
			Smooth Aluminum Surface					
214	20.1		10.0	1.88	0.089	6440	1.570	0.0062
215	20.0		4.8	1.77	0.063	4303	1.561	0.0062
216	20.1	0.25	40.5	2.13	0.168	13769	1.294	0.0059
217	20.1		23.9	1.82	0.140	9802	1.212	0.0061
218	20.1		15.5	1.63	0.119	7449	1.174	0.0062
219	20.1		9.9	1.46	0.100	5620	1.150	0.0061
220	20.1		4.9	1.39	0.070	4026	1.158	0.0067
221	19.2	0.125	40.7	1.72	0.187	12267	1.000	0.0055
222	19.2		27.4	1.51	0.164	9335	0.927	0.0058
223	19.3		16.9	1.36	0.136	7006	0.921	0.0057
224	19.3		9.4	1.28	0.105	5076	0.983	0.0061
225	19.1		5.2	1.07	0.085	3429	0.916	0.0063
226	19.9	0.0625	40.7	1.52	0.199	11605	0.850	0.0047
227	19.8		24.6	1.47	0.167	9392	0.898	0.0048
228	19.6		16.3	1.17	0.144	6438	0.769	0.0048
229	19.4		9.6	1.02	0.119	4575	0.735	0.0049
230	19.2		5.4	0.96	0.092	3345	0.789	0.0052
			715-Micron Sand Surface					
231	18.8	2.0	40.2	3.23	0.136	16447	2.181	0.0096
232	19.0		24.6	2.95	0.111	12261	2.205	0.0092
233	19.0		14.0	2.44	0.092	8414	2.004	0.0099
234	19.0		10.5	2.27	0.083	7062	1.967	0.0098
235	19.0		4.1	1.86	0.057	3982	1.947	0.0099
236	20.2	1.0	39.3	2.57	0.151	14955	1.650	0.0092
237	20.2		24.3	2.26	0.126	10984	1.590	0.0092
238	20.3		16.4	2.06	0.109	8676	1.550	0.0092
239	19.0		11.4	1.82	0.096	6559	1.468	0.0095
240	19.0		5.0	1.55	0.069	4018	1.476	0.0090
241	20.0	0.50	40.4	2.20	0.168	13518	1.258	0.0084
242	19.9		23.8	1.84	0.138	9744	1.236	0.0085
243	19.6		15.9	1.65	0.120	7556	1.188	0.0086
244	19.6		9.6	1.47	0.099	5557	1.165	0.0085
245	19.6		4.6	1.31	0.072	3606	1.218	0.0078
246	19.1	0.25	39.6	1.74	0.184	12043	1.011	0.0077
247	19.1		23.2	1.53	0.150	8613	0.982	0.0077
248	19.3		15.1	1.59	0.126	7584	1.118	0.0075
249	19.4		9.1	1.27	0.116	5211	0.969	0.0078
250	19.4		4.9	1.12	0.080	3404	0.992	0.0089
251	19.1	0.125	39.8	1.54	0.196	11372	0.868	0.0064
252	19.2		24.3	1.36	0.163	8382	0.840	0.0064
253	19.2		15.2	1.19	0.138	6203	0.798	0.0066
254	19.1		10.7	1.10	0.120	5975	0.793	0.0068
255	19.0		4.2	0.85	0.096	3090	0.690	0.0069
256	18.1	0.0625	40.2	1.37	0.208	10564	0.754	0.0063
257	18.5		28.2	1.25	0.183	8533	0.732	0.0063
258	18.8		18.0	1.15	0.161	7042	0.724	0.0062
259	19.1		10.5	0.94	0.128	4585	0.694	0.0065
260	18.5		4.2	0.81	0.087	2654	0.694	0.0066

TABLE 2 (CONTINUED)

Test No.	Temp. C°	Slope %	Rate of flow gpm	Velocity fps	Depth ft.	Reynolds number	Froude number	Manning's n
			Smooth Aluminum Surface					
261	19.4	2.0	41.2	2.62	0.152	17168	1.488	0.0146
262	20.0		26.4	2.56	0.130	13970	1.491	0.0146
263	20.0		16.2	1.93	0.111	9282	1.449	0.0140
264	20.0		10.2	1.68	0.095	7131	1.356	0.0145
265	19.8		5.2	1.44	0.073	4506	1.325	0.0148
266	20.0	1.0	40.4	2.07	0.169	14634	1.170	0.0141
267	20.1		26.2	1.82	0.145	11288	1.106	0.0144
268	20.3		23.8	1.72	0.142	9555	1.151	0.0140
269	20.4		12.7	1.41	0.125	8380	0.898	0.0142
270	20.0		3.6	0.96	0.075	2773	0.821	0.0143
271	20.5	0.5	41.2	1.68	0.190	12554	0.973	0.0124
272	20,8		24.4	1.42	0.159	8910	0.894	0.0120
273	20.8		14.0	1.23	0.130	6274	0.850	0.0122
274	20.9		8.9	1.04	0.112	4600	0.879	0.0130
275	21.0		4.1	0.99	0.078	3074	0.897	0.0126
276	21.1	0.25	40.4	1.40	0.207	11440	0.768	0.0114
277	21.2		25.3	1.21	0.176	8462	0.721	0.0112
278	21.1		12.7	0.98	0.138	5363	0.662	0.0112
279	21.1		9.7	0.91	0.125	4521	0.646	0.0113
280	21.2		4.2	0.76	0.091	2752	0.630	0.0118
281	21.1	0.125	40.4	1.23	0.221	10743	0.654	0.0087
282	21.0		24.3	1.06	0.185	7680	0.613	0.0090
283	21.1	0.125	14.9	0.92	0.155	5631	0.583	0.0092
284	21.0		9.6	0.80	0.133	4701	0.616	0.0095
285	21.2		4.1	0.60	0.097	2525	0.525	0.0094
286	21.5	0.0625	40.7	1.13	0.230	10427	0.592	0.0068
287	20.2		25.0	0.93	0.199	7360	0.522	0.0076
288	20.0		15.7	0.85	0.165	5424	0.524	0.0073
289	20.0		9.4	0.73	0.138	3919	0.595	0.0075
290	20.0		5.6	0.65	0.112	2823	0.488	0.0074

Knox Silt Loam with Infiltration

Test No.	Temp. C°	Slope %	Rate of flow gpm	Velocity fps	Depth ft.	Infiltration rate in./hr.	Reynolds number	Froude number	Manning's n
291	20.2	1.0	4.2	1.50	0.053	1.32	3364	1.542	0.0211
292	20.2		2.9	1.02	0.046	1.42	2418	1.185	0.0200
293	20.2		2.2	0.76	0.045	1.42	1796	0.898	0.0201
294	20.0		0.9	0.48	0.036	1.36	906	0.628	0.0202
295	19.3		0.4	0.41	0.027	1.38	418	0.468	0.0210
296	21.8	0.50	4.6	0.89	0.071	1.51	2864	0.741	0.0149
297	21.8		3.0	0.69	0.059	1.60	2265	0.709	0.0160
298	21.6		2.4	0.64	0.051	1.48	1790	0.716	0.0152
299	21.3		0.8	0.33	0.037	1.51	915	0.431	0.0168
300	21.2		0.4	0.30	0.031	1.50	425	0.360	0.0160

TABLE 2 (CONTINUED)

Test No.	Temp. C°	Slope %	Rate of flow gpm	Velocity fps	Depth ft.	Infiltration rate in./hr.	Reynolds number	Froude number	Manning's n
301	20.5	0.25	10.5	0.75	0.120	0.90	4226	0.539	0.0153
302	20.8		6.7	0.66	0.098	0.90	3223	0.528	0.0155
303	20.8	0.25	4.3	0.60	0.078	1.01	2855	0.562	0.0159
304	20.6		2.2	0.49	0.059	1.02	1512	0.506	0.0164
305	20.2		0.7	0.31	0.042	1.01	577	0.324	0.0168
306	20.0	0.125	11.2	0.63	0.137	1.03	4044	0.431	0.0137
307	20.0		6.2	0.57	0.105	1.04	2810	0.436	0.0132
308	20.0		4.1	0.50	0.087	1.08	2166	0.419	0.0139
309	21.0		1.8	0.44	0.054	1.07	1286	0.476	0.0132
310	19.5		1.5	0.35	0.047	1.10	551	0.405	0.0136
311	21.0	0.0625	11.3	0.50	0.146	0.91	4456	0.382	0.0128
312	21.0		5.7	0.48	0.109	0.92	2947	0.374	0.0129
313	21.0		5.5	0.47	0.108	0.94	2550	0.367	0.0121
314	21.0		4.4	0.44	0.095	0.94	2333	0.367	0.0122
315	21.0		2.2	0.33	0.075	1.01	1332	0.310	0.0130

Knox Silt Loam without Infiltration

Test No.	Temp. C°	Slope %	Rate of flow gpm.	Velocity fps	Depth ft.	Reynolds number	Froude number	Manning's n
316	19.3	0.25	10.7	0.78	0.120	4628	0.561	0.0146
317	19.2		8.2	0.71	0.107	4250	0.544	0.0163
318	19.7		4.3	0.63	0.078	3748	0.513	0.0159
319	19.1		2.9	0.57	0.067	1924	0.453	0.0151
320	19.0		1.0	0.31	0.045	687	0.367	0.0159
321	19.0	0.125	11.7	0.71	0.133	4203	0.488	0.0130
322	19.0		8.8	0.66	0.117	3500	0.480	0.0131
323	19.0	0.125	6.9	0.62	0.102	2835	0.460	0.0138
324	19.4		3.4	0.51	0.078	1990	0.455	0.0126
325	19.7		1.0	0.30	0.048	1322	0.305	0.0140
326	18.6	0.0625	12.3	0.64	0.142	4050	0.442	0.0120
327	19.0		8.2	0.58	0.119	3314	0.434	0.0126
328	19.1		4.3	0.50	0.091	2300	0.433	0.0124
329	19.3		1.9	0.37	0.062	1107	0.387	0.0126
330	18.8		0.7	0.18	0.043	437	0.235	0.0128